Topographic analysis and Weibull regression for prediction of strain localisation in an automotive aluminium alloy

J. B. Hubbard[1], M. R. Stoudt*[1] and A. M. Possolo[2]

We fit a two-parameter Weibull regression model by maximum likelihood estimation (MLE) to filtered surface roughness data. These data were acquired with scanning confocal laser microscopy performed on aluminium alloy AA 5754-O surfaces that were subjected to a range of plastic strain intensities in three different in-plane strain modes. Noting that one of the two Weibull regression parameters is, to a good approximation, invariant with strain intensity for a given strain mode, the authors find that the variation of the second parameter with strain intensity conforms to a simple quadratic function. These functions may then be used to generate accurate, statistically significant, single parameter predictors of both strain intensity and strain mode up to and including the onset of critical strain localisation and/or failure.

Keywords: Strain localisation modelling, Strain mode, Scanning laser confocal microscopy, 3D characterisation, Weibull statistics, Sheet metal forming

Introduction

The need to reduce gross vehicle weight and improve fuel economy has escalated the demand for new lightweight materials such as aluminium alloys, magnesium alloys and advanced high strength steel throughout the transportation industry. However, the available property data and constitutive laws for these new materials are often limited or inadequate for use in the numerical models that are used to predict the behaviour during sheet metal forming. The ensuing inability to reliably model the mechanical behaviour creates significant obstacles that impede widespread incorporation of new alloys. Inaccurate prediction of the manner in which surface inhomogeneities evolve during sheet metal forming is a prime example of the problem. In addition to creating a surface that is cosmetically unacceptable, surface inhomogeneities have profoundly detrimental effects on the formability of the metal sheet. Specifically, they generate unpredictable variability in the friction between the metal sheet and the die surfaces during stretch forming, and they promote strain localisation, both of which lead to unexpected failures in the sheet metal component.[25] For this reason, the character of the deformed surface can essentially determine whether an alloy is suitable for a particular application.

During sheet metal forming, macroscopic deformation occurs through a complex combination of strain modes (e.g. biaxial, uniaxial and plane strain). Since each strain mode imposes specific constraints on the material flow during stretch forming, each mode imparts distinctly different surface morphologies for the same overall level of plastic strain.[23] Thus, it is essential that the deformation produced by each component of the macroscopic strain be properly identified and accurately characterised. Such characterisations tend to be expensive and complicated processes that require numerous high resolution measurements of the deformation under each strain mode.[13] Despite all of the many improvements in the numerical models currently adopted by the US automotive industry to predict the evolution of the deformed surface,[1,6–8,15,19,21,27] inconsistencies still exist between the results predicted by these models and what is observed experimentally. This creates a situation where a numerical model that predicts the material behaviour during forming may correctly indicate the overall trends of the deformation, but fails to reliably predict the actual magnitudes of the strain at which critical localisation (failure) occurs.[9]

It was recently noted[23] that a two-parameter Weibull probability distribution, in which α is the scale parameter and β is the shape parameter, provides good overall fits to filtered surface roughness data. These roughness data were acquired from the surfaces of aluminium alloy AA 5754-O specimens that were subjected to a range of plastic strain intensities in three different in-plane strain modes. The authors refer to this data as filtered because they analysed raw topographic data with a technique that extends the profile based peak to valley surface roughness parameter Rt to a matrix form. This process generated sets of local intensity maps composed of coarse grained ($n \times n$) arrays of Rt 'cells' that were constructed from the raw topographic data.

The maximum height of a profile, Rt, is defined in the surface roughness literature as the vertical distance between the highest and the lowest points within a profile of any given length[3]

[1]NIST Centre for Metal Forming, Materials Science and Engineering Laboratory, Gaithersburg, MD 20899, USA
[2]Statistical Engineering Division, Information Technology Laboratory, National Institute of Standards and Technology, 100 Bureau Drive, Gaithersburg, MD 20899, USA

*Corresponding author, email stoudt@nist.gov

$$Rt = Rp + Rv \qquad (1)$$

In this equation, Rp is the vertical distance between the highest point of the profile and the mean line, and Rv is the vertical distance between the lowest point of the profile and the mean line within the same evaluation length. Note that the data located below the mean line of the profile are traditionally given a negative sign, so by this convention, all of the Rt values are positive.

The Rt parameter demonstrates several attractive properties that make it ideal to characterise the surface conditions that promote critical strain localisation, and to quantify the relative magnitudes of those surface conditions:

(i) it is highly sensitive to local changes in surface height

(ii) it is based on a straightforward calculation

(iii) the data over which Rt is determined can range from a short profile segment to the entire profile. Consequently, the Rt parameter can track the changes in the surface height on a local or on an overall basis

(iv) the magnitudes of the local surface extremes will change with strain to the point where they reflect the onset of critical strain localisation

(v) the Rt parameter can be easily determined between any two points or nodes during a numerical simulation, thereby making changes in the local surface conditions directly integrable into formability models.

Mathematically, an Rt matrix is analogous to a Euclidean distance matrix.[10] Construction of an Rt matrix required subdividing the original 512 row × 512 column matrix of height data into a 128 row × 128 column array of Rt 'cells.' Each element in the 16 384 cell Rt matrix, $Rt_{(i,j)}$, is the maximum difference for the set of 16 height values contained within each (4 row × 4 column) cell. While similar in concept to the profile form, the matrix format preserves the spatial coordinates for each $Rt_{(i,j)}$ cell by construction. Therefore, this approach enables direct quantification of the local Rt magnitudes as well as the specific location of that Rt value within the original topography. That is, this technique directly links any discernible feature in the source topography to the corresponding change in magnitude of the local surface height. Obviously, the level of resolution can easily be adjusted by simply changing the dimensions of the submatrix cells. For this reason, this process was repeated using larger (64 element 8 × 8 cells) to evaluate the strength of the resolution dependence in the Rt data.

An example of this construction exhibiting the relationships between the original topography (Fig. 1*A*), the distribution of surface heights in the topography (Fig. 1*B*), the corresponding Rt map (Fig. 1*C*) and the distribution of filtered surface heights (Fig. 1*D*) is shown as Fig. 1. Each cell in the Rt map (Fig. 1*C*) is derived from the topography (Fig. 1*A*) and it accentuates the height disparities between topographical features. As such, this approach generates a direct three-dimensional quantification of the local intensities produced by a change in the surface morphology. Since maps were constructed for multiple strain levels in three different strain modes, one can evaluate the morphological conditions that promote critical strain localisation for each strain condition.

It was noted in Refs. 22 and 23 that the Weibull α parameter seems to vary systematically with strain mode and strain intensity, and that the Weibull β parameter was essentially constant for each strain mode. For this reason, the Weibull β parameter could possibly be regarded as a characteristic of the AA 5754 alloy in the O condition. In the present paper, the authors attempt to quantify these general observations and to ascertain the extent to which the Weibull scale parameter α can serve as a predictor of the strain intensity up to and including the onset of critical strain localisation and/or failure. The existence of an isomorphism (i.e. a one to one relationship) between the strain mode, the strain intensity and a Weibull regression scale parameter, would strongly suggest an empirical correlation between these Rt maps and the active deformation mechanisms for this particular alloy.

Experimental

Sets of 30 × 30 cm (12 × 12 in.) blanks were sheared from commercially available 1 mm thick AA 5754-O sheet stock for testing. This aluminium alloy was developed primarily for automotive applications, and like most alloys in the 5xxx series, AA 5754 is substitutionally strengthened, and it demonstrates good overall formability. The literature indicates that AA 5754 typically contains 2·8 mass%Mg for solid solution strengthening, and ~0·5 mass%Mn for grain refinement and stability.[4] The grain structure was relatively equiaxed in the rolling plane and slightly elongated along the rolling direction of the sheet, which is indicative of the recrystallised microstructure normally associated with the O temper. The grain size for this alloy was 40 ± 20 μm.[5] All of the specimens used for this evaluation were polished to a 6 μm diamond finish using standard metallographic practice to better reveal the surface character at low strains and to produce more consistent surface roughness measurements.

After polishing, the blanks were deformed in three in-plane proportional strain modes, which are traditionally defined in terms of the ratio of in-plane principal strains: $\rho = \varepsilon_2/\varepsilon_1$.[14] The first strain mode was equibiaxial ($\rho = 1$). The second strain mode was uniaxial ($\rho = -0·5$), and the third was plane strain ($\rho = 0$). Both the equibiaxial and plane strain deformations were imposed using an augmented[20] Marciniak flat bottom ram test.[16] Samples were strained in equibiaxial tension using a typical strain rate of 5×10^{-4} s^{-1} to 5, 10, 15 and 20% nominal true strain. The uniaxial samples were all machined to an ASTM E08-91 standard sheet type tensile specimen geometry and then strained to nominal true strain values of 5, 10 and 15% using standard test methods[2] with a constant displacement rate resulting in an average strain rate of 6×10^{-4} s^{-1}. A third set of samples was strained to similar true strain levels in the plane strain condition.

One sample was taken to 'failure' in each strain mode. In this case, the term 'failure' denotes the maximum uniform strain outside of the region where critical localisation occurred. Note that the actual fracture event is not included in any of the topographic measurements at the failure strain level. For this reason, the surface roughness data acquired from these samples are the maximum roughness values that can be generated uniformly in the AA 5754-O alloy by each strain mode. These data also reflect the surface conditions that produced the failure event. Coupons were cut from the centre of each deformed specimen for topographic analysis.

The surfaces were quantified for each strain condition with scanning laser confocal microscopy (SLCM). Each
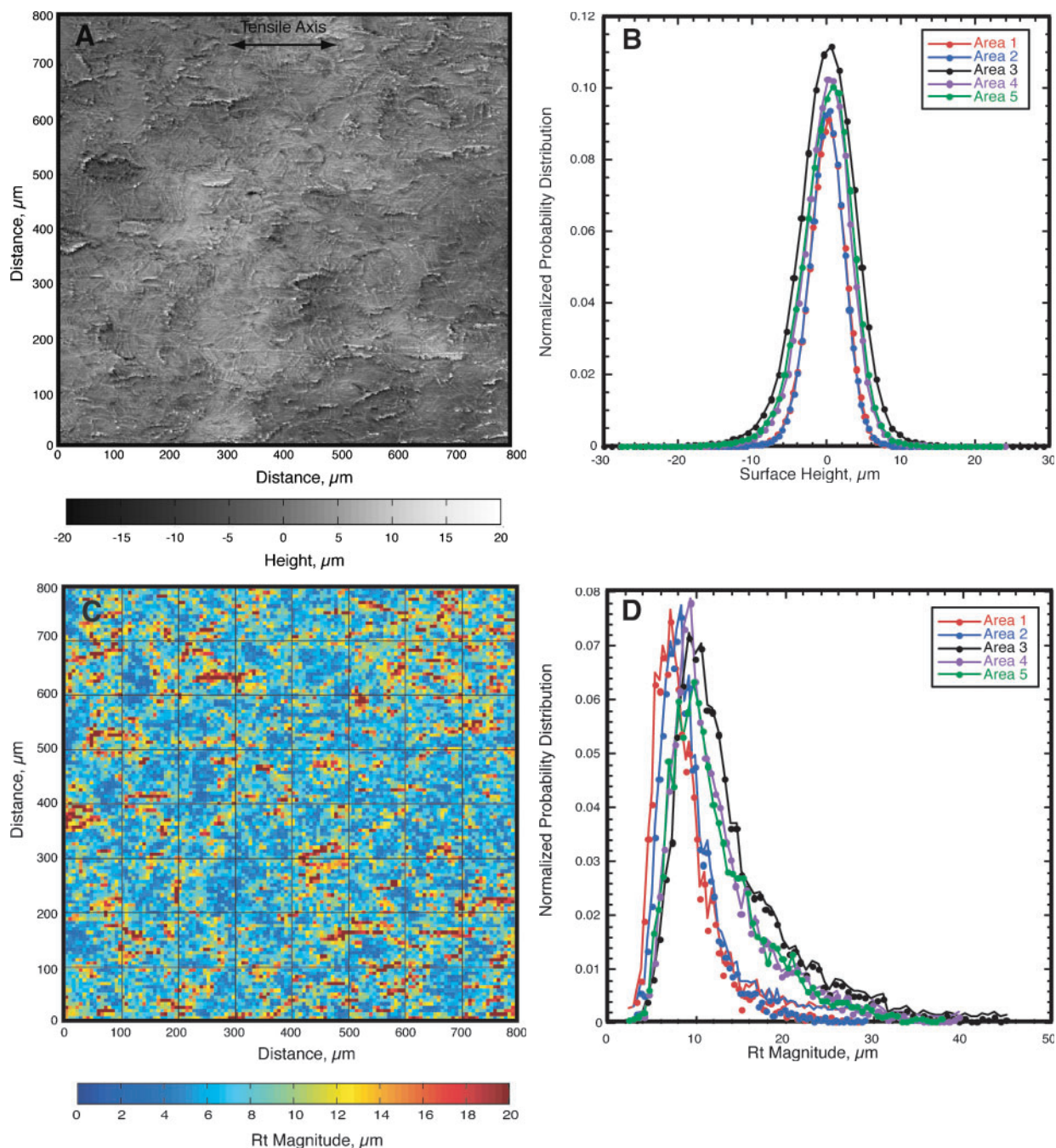
A topography of AA 5754-O at maximum uniform strain condition in uniaxial strain mode; B corresponding distribution of surface heights for each of five areas sampled in this strain condition; C Rt map constructed from topography shown in A; D corresponding distribution of Rt values for each of five Rt maps

1 Series of figures illustrating relationships between topography, Rt maps and Weibull distribution used to evaluate and model Rt data

topographic measurement consisted of acquiring five well separated SLCM images of the specimen surface using a ×10 objective lens and a nominal z-scan depth of ~40 μm. These imaging conditions generated sets of 640 × 512 pixel intensity images acquired with 12 bit resolution and were consistent for all measurements. The spacing between sampling points in the (x,y) plane was fixed by the objective lens at 1·56 μm, and the spacing between the individual focal planes within each image was ~100 nm. These conditions yielded nominal physical dimensions (x,y,z) of 1000 × 800 × 40 μm for each image. As described in Ref. 24, the SLCM stores each topographic image data as a raw depth map in tagged image file format (TIFF), which contains the

complete set of imaging parameters and binary pixel values. A computer code utilising the format standards within these TIFF images was developed to convert the raw depth map into a simple numerical matrix of surface heights. The resulting matrix was then trimmed to a square 512 row × 512 column array to facilitate the matrix based mathematical operations. Using the aforementioned x–y pixel spacing, the values in each matrix correspond to an 800 × 800 μm area of the surface.

After conversion, the extreme values (defined as the values in the height data greater than $\pm 6\sigma$, where σ is the standard deviation for all the heights in that matrix) were screened from the datasets. This step was required because some of the statistical parameters used to

interpret the surface data are highly sensitive to outlier data points. Any individual Rt value that exceeded the $\pm 6\sigma$ threshold was reset to the mean value for that particular surface. Note that the number of affected data points for a given surface was typically less than 20 points (or <0·008% of the total number of data points within the matrix). The resulting sets of residual matrices were used as the source for all subsequent assessments of the surface character. Note that it was essential for these images to be well separated to ensure that the surface data contained in each image was statistically independent (i.e. no overlapping image data), and that the data properly represented the full range of surface characteristics.[24]

Results and discussion

Weibull regression

The authors modelled the dispersion of the Rt values using Weibull probability distributions in which the scale parameter is expressed as an explicit function of the strain intensity. This model is often called a Weibull Regression, a special case of survival regression, which is widely used in studies of reliability. Such a model is appropriate when one wishes to describe how the lifetime of a mechanical part depends on one or several attributes (either qualitative or quantitative).

The Weibull probability density $p_{\alpha,\beta}$ is defined as

$$p_{\alpha,\beta}(r) = \left(\frac{\beta}{\alpha}\right)\left(\frac{r}{\alpha}\right)^{\beta-1}\exp\left[-\left(\frac{r}{\alpha}\right)^{\beta}\right] \quad (2)$$

for any Rt value $r>0$, and fixed values of the scale ($\alpha>0$) and the shape ($\beta>0$) parameters. Given a sample of Rt values ($r_1, \ldots, r_m$), the maximum likelihood estimates (MLEs) of the scale and shape parameters $\hat{\alpha}$ and $\hat{\beta}$ (the hats denote MLE values), maximise the product $p_{\alpha,\beta}(r_1)$, $p_{\alpha,\beta}(r_2)$, $\ldots, p_{\alpha,\beta}(r_m)$ of the likelihood function L with respect to the Weibull α and β parameters for a given strain mode.[17]

The method of maximum likelihood is one of several statistical methods that can be used for estimating parameter values from empirical data. However, when it is applicable, MLE is generally preferred over other methods because MLEs have attractive statistical properties. In addition, the maximum likelihood estimation process also produces approximate assessments of the parameter uncertainties. When the empirical data are similar outcomes of independent Weibull random variables, all with the same values of α and β, the MLEs can be found by solving a system of two non-linear equations, $\partial L/\partial\alpha=0$, and $\partial L/\partial\beta=0$, where L, the logarithm of the likelihood function, is defined as

$$L(\alpha,\beta)=m\log\left(\frac{\beta}{\alpha}\right)+(\beta-1)\sum_{i=1}^{m}\log\left(\frac{r_i}{\alpha}\right)-\sum_{i=1}^{m}\left(\frac{r_i}{\alpha}\right)^{\beta} \quad (3)$$

Alternatively, the MLEs can be found by maximising L directly, which is what was carried out in this case, using Nelder–Mead's[18] algorithm as implemented in function 'optim' of the R programming environment for statistical analysis and graphics.[26]

The Rt values in this evaluation are not necessarily statistically independent because the Rt values in neighbouring cells tend to be positively correlated. That is, if an individual cell has an Rt value larger than the median Rt value, then it is highly likely that a neighbouring cell will also have a similarly large Rt value. Therefore, even though the parameter estimates will be optimised by the MLE technique, the associated uncertainty assessments, which are based on the assumption of statistical independence, will tend to underestimate the magnitude of the actual uncertainties.

The measured strain values are expressed as nominal true strain values, as equivalent scalar modal true strain values $\varepsilon_{\text{modal}}$ (where modal denotes either equibiaxial, uniaxial or plane strain and is equivalent to ε_{11} in the table), and as effective true strain values ε_{eff} (where the effective strain is the magnitude of a modal strain expressed in terms of the equivalent uniaxial strain) in Table 1. The effective strain is typically determined from the principal components of the modal strain tensor (i.e. ε_{11}, ε_{22} and ε_{33} in Table 1 and the von Mises criterion[11]

$$\varepsilon_{\text{eff}}=\frac{(2)^{1/2}}{3}\left[(\varepsilon_{11}-\varepsilon_{22})^2+(\varepsilon_{22}-\varepsilon_{33})^2+(\varepsilon_{11}-\varepsilon_{33})^2\right]^{1/2} \quad (4)$$

The authors have found that the maximum likelihood estimate of the Weibull scale parameter $\hat{\alpha}$ varies markedly and systematically with strain intensity within each strain mode. That is, while the magnitude of $\hat{\alpha}$ is proportional to the strain intensity, the manner in which $\hat{\alpha}$ varies depends on the macroscopic constant volume constraints imposed by the individual strain modes. In contrast, the overall magnitude of the maximum likelihood estimate for the Weibull shape parameter $\hat{\beta}$

Table 1 Strain levels achieved during in-plane deformation: effective strains were calculated using von Mises criterion (equation (4))[11]

Nominal true strain	$\varepsilon_{\text{modal}}\equiv\varepsilon_{11}$	ε_{22}	ε_{33}	ε_{eff}
Equibiaxial				
0·05	0·049	0·051	−0·106	0·104
0·10	0·097	0·097	−0·216	0·210
0·15	0·140	0·139	−0·278	0·279
0·20	0·200	0·199	−0·412	0·408
0·25	0·258	0·254	−0·638	0·512
Uniaxial				
0·05	0·051	…	…	0·051
0·10	0·116	…	…	0·116
0·15	0·166	…	…	0·166
0·20	0·228	…	…	0·228
Plane strain				
0·05	0·051	−0·002	−0·064	0·066
0·10	0·100	−0·008	−0·089	0·109
0·15	0·147	−0·001	−0·145	0·169
0·20	0·158	−0·003	−0·207	0·181
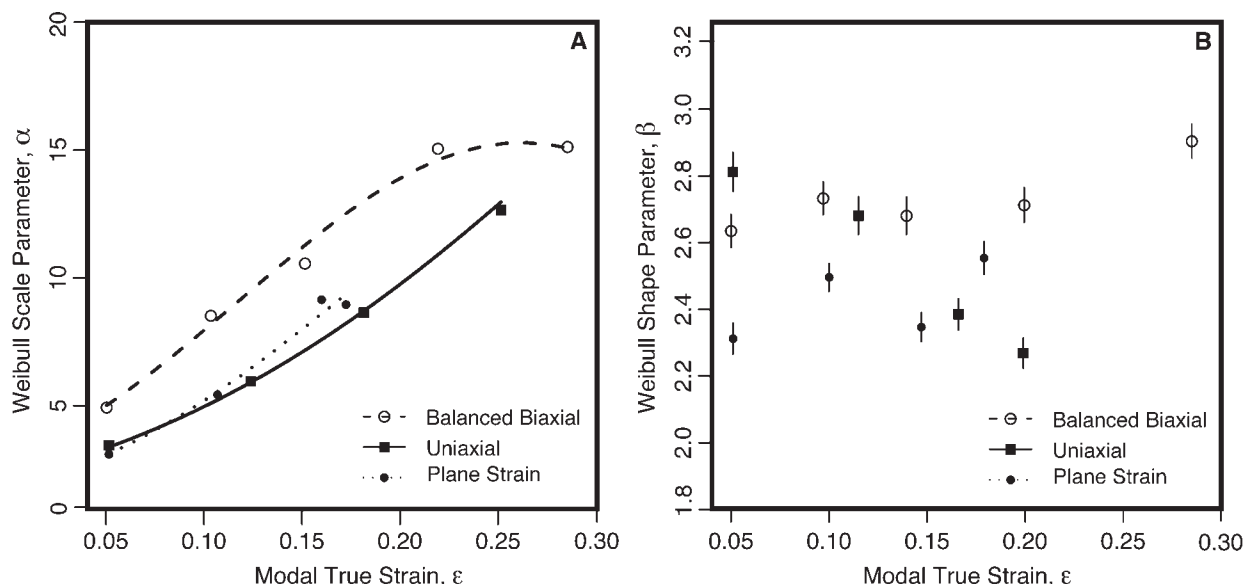
A Weibull scale parameter α as function of modal true strain; *B* Weibull shape parameter β as function of modal true strain

2 Magnitudes of Weibull parameters estimates calculated for set of Rt values based on 64×64 maps

remains essentially constant with strain intensity for a given strain mode. However, the relative magnitudes of the $\hat{\beta}$ values do exhibit slight differences between the three strain modes. Because of the relative insensitivity of $\hat{\beta}$ to changes in strain, and given the approximately quadratic trend of the values of $\hat{\alpha}$ as a function of ε, the authors model these as

$$\log(\alpha) = \gamma_0 + \gamma_1 \varepsilon + \gamma_2 \varepsilon^2 \qquad (5)$$

In these circumstances, the likelihood function L becomes a function of four parameters, β, γ_0, γ_1 and γ_2. The values of these parameters that maximise the likelihood function are the maximum likelihood estimates $\hat{\beta}, \hat{\gamma}_0, \hat{\gamma}_1$ and $\hat{\gamma}_2$.

Figures 2 and 3 exhibit the results of the Weibull regression model fits to the Rt data, using the modal strain intensity, separately for each particular strain mode. The plots shown in Fig. 2 are derived from the set of Rt maps produced by the 64×64 cell format. Similar plots, as shown in Fig. 3, are derived from the set of Rt maps produced by the 128×128 cell format.

The lines in Figs. 2*A* and 3*A* exhibit how α varies with the set of strain intensities determined from each set of modal strain values (for the 64×64 and the 128×128 cases respectively). While the α magnitudes are somewhat greater in Fig. 2*A*, the patterns of the relationships are strikingly similar to those shown in Fig. 3*A*. Each plot symbol represents the value of $\hat{\alpha}$ derived from all five regions sampled on an individual coupon. Data were pooled across all five regions because each topographic sample has the same nominal strain intensity. The uncertainty in the vertical placement of each plotted symbol in Figs. 2*A* and 3*A* (and also in both panels of Fig. 4) is the uncertainty of $\hat{\alpha}$ that derives from the dispersion of Rt values within and between regions in the same coupon. The magnitudes of these uncertainties are roughly comparable to the sizes of the plot symbols and are not visible in these figures. Note that the curved lines shown in these figures are not fitted to the points. The lines result directly from the Weibull regression. The

points, which represent the MLEs derived for each value of strain intensity (and strain mode) separately, are included to emphasise that the model is not a perfect fit. Figure 4 shows the behaviour of α as a function of the effective true strain. Since the effective strain is an estimate of the uniaxial strain component in each strain mode, this figure enables a direct comparison of the α behaviour with respect to a common strain intensity.

Each point in Figs. 2*B* and 3*B* illustrates how β varies with the same set of modal strain intensities. The corresponding plots for the β estimates as a function of the effective strain are qualitatively comparable to those shown in Figs. 2*B* and 3*B*. The superimposed thin vertical lines shown in these plots represent the 95% confidence intervals for β. These confidence intervals are based on standard uncertainties derived from a simulation study that was performed to account for the fact that the Rt values are not statistically independent. More precisely, the authors took the following steps to estimate the standard uncertainty of the maximum likelihood estimate of β for each modal strain intensity value. First, the authors modelled the logarithms of the Rt values as a Gaussian random field on a regular lattice (based on either the 64×64 or 128×128 maps), with Matern's covariance function.[12] Second, the authors used the parameters of the fitted model to simulate 1000 realisations of arrays of Rt values, to which the authors fitted the Weibull probability distributions described above. Third, the authors computed the standard deviation of the resulting $\hat{\beta}$ values. This approach provides a more conservative and accurate assessment of the true uncertainties in the β parameter estimates. The results revealed that the standard deviations of the $\hat{\beta}$ values produced by the simulation are approximately twice as large as the standard deviations that were based on the assumption that the Rt values are statistically independent.

When the confidence intervals of all the β values within a particular strain mode are projected onto the vertical axis in either Fig. 2*B* or Fig. 3*B*, an overlap between two or more intervals indicates that the values of β corresponding to those strain intensities are
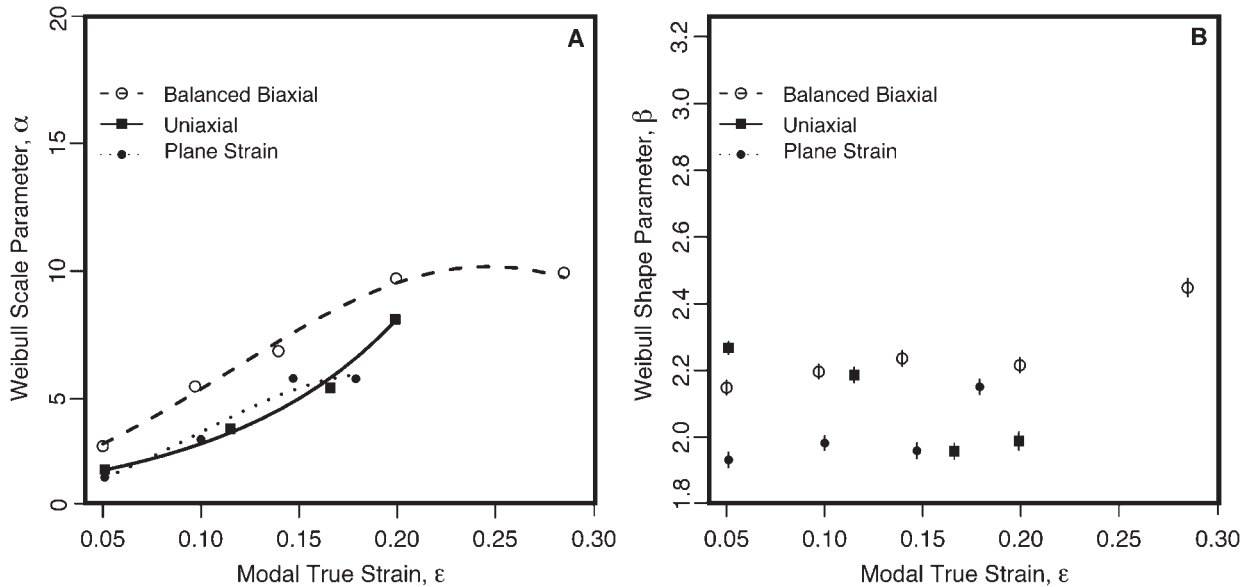
A Weibull scale parameter α as function of modal true strain; *B* Weibull shape parameter β as function of modal true strain

3 Magnitudes of Weibull parameters estimates calculated for set of Rt values based on 128 × 128 maps

statistically indistinguishable. Even when the β values do not overlap (i.e. they are significantly different statistically), the relative magnitude of the differences between these β values is quite small with respect to the magnitude of the changes in the α values for the same strain intensities. For this reason, the variability in the β values is of little consequence from an engineering perspective.

Strain prediction

The Weibull regression models fitted to the Rt data are all highly statistically significant, in that the Weibull parameters and the coefficients in the quadratic regression fit in equation (5) are statistically non-negligible. This implies that the fitted Rt values are a relevant predictor of strain intensity for the three strain modes considered in this study. Furthermore, the Rt values

retain their predictive value whether they are expressed as either modal or effective strains. To illustrate how the models used in this evaluation can be used to derive predictions of strain intensity information from a set of roughness data, consider the specimen that was strained in uniaxial tension to produce a strain intensity of $\varepsilon_{modal}=0 \cdot 116$ as an example. The Weibull MLEs calculated for one of the five sets of Rt values from this coupon were $\hat{\alpha}=6 \cdot 526$ and $\hat{\beta}=2 \cdot 896$ (note that in Figs. 2 and 3, there is only one point representing the MLE for each combination of strain intensity and strain mode because, as indicated above, the Rt data from all five coupons were pooled to estimate the MLEs shown). The Weibull regression produced the following fit for this strain intensity for this particular strain mode

$$\log(\alpha) = 0 \cdot 8487 + 6 \cdot 633\varepsilon_{modal} + 9 \cdot 321\varepsilon_{modal}^2$$
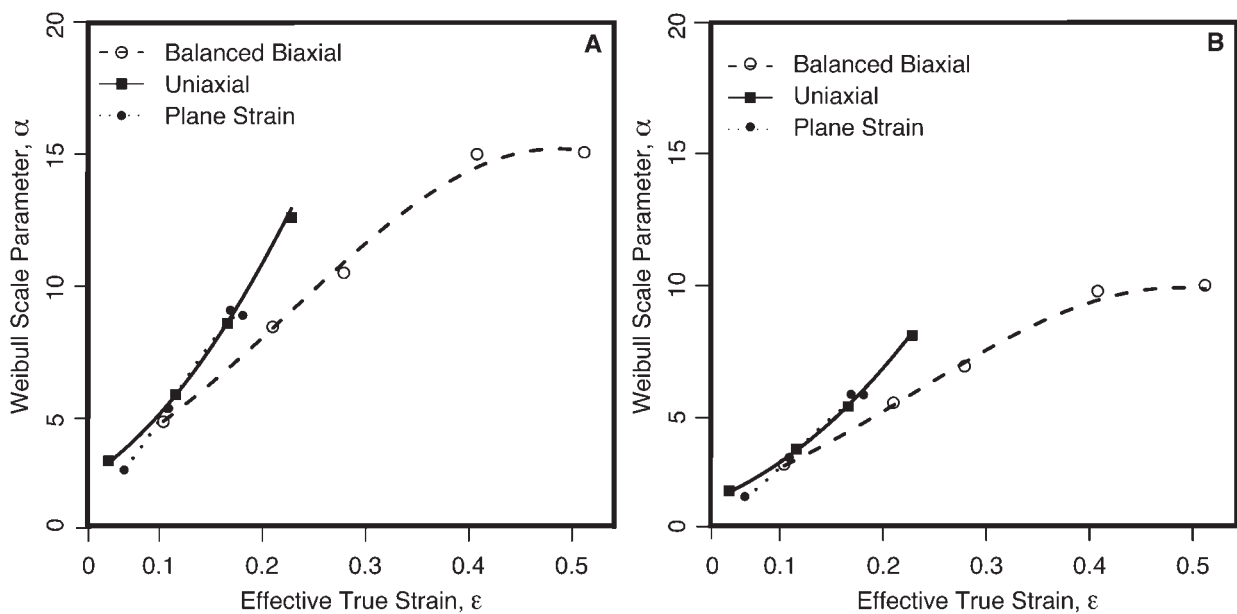
A α values calculated from set of 64 × 64 maps; *B* α values calculated from set of 128 × 128 maps

4 Magnitudes of Weibull scale parameters shown as function of effective true strain

Substituting the $\hat{\alpha}$ value of 6·526 into this expression and solving for ε_{modal} produces a result of $\varepsilon_{modal} = 0·13$. Similar calculations produce estimates of ε_{modal} for the remaining four surface measurements for this particular strain intensity: 0·11, 0·12, 0·11 and 0·12. These results suggest that in this example, there is little variability in the strain intensity between regions of the same coupon.

It should be re-emphasised that the following simplifying assumptions were made to enable the application of Weibull regression analysis to these data:[17] the shape parameter β remains invariant with strain intensity for each strain mode and the α parameter and the strain intensity are related as described by equation (3). This model is advantageous because it allows for integration of the information from each surface measurement, irrespective of the strain intensity, which corresponds to a particular strain mode.

The differences in magnitudes of α and β produced from the two sets of Rt maps (64×64 and 128×128) demonstrate that the filtering and the binning of the data have some influence on the behaviour of both α and β. That is, the values of α and β both exhibit some resolution dependence. However, the similarities in the overall trends of these two parameters across the two different resolutions suggest that they reflect characteristics of the material as a whole. Therefore, the key question raised by these results is whether this predictive capability only holds for this specific alloy and heat treatment, or whether it might be more generally applicable. If the latter possibility turns out to be valid, this approach could provide a basic methodology for constructing a fundamental constitutive relationship between surface roughness and strain. Such a relationship could have substantial practical relevance. To determine the answer, it is necessary to ascertain whether the Weibull shape parameter β remains approximately invariant for any or all of the strain modes after implementing a change in a material characteristic of this alloy that has a strong influence on the mechanical properties, such as the grain size, the workhardening behaviour or the crystallographic texture. It is also of particular interest to determine whether the β parameter demonstrates a similar approximate invariance in a different alloy system. If β were to demonstrate approximate invariance and α were to scale with strain intensity monotonically under either of these conditions, it may then be possible to use surface roughness measurements straightforwardly to determine the principal components of the strain tensor (i.e. ε_{11}, ε_{22} and ε_{33}) in each strain mode. Such a constitutive relationship could prove to be quite useful as a predictive tool in sheet metal forming.

Conclusions

In the present paper, the authors have shown that a Weibull regression, fitted using the method of maximum likelihood, is an appropriate model for the Rt values that were derived from topographic measurements on strained coupons of AA 5754. The results also indicated that the Weibull model could be used to develop an accurate parametric predictor of strain intensity for a given set of Rt data. Even though the differences observed between the 64×64 Rt maps and the 128×128 Rt maps revealed that the behaviour of the

Weibull scale and shape parameters are somewhat dependent on the Rt cell size, the similarities in the general trends suggest that these parameters are likely to be characteristics of the material as a whole.

The critical issue raised with this analysis is whether the Weibull parameters will demonstrate the same characteristics that were observed here in a different alloy. That is, shape parameter is approximately invariant, and the scale parameter scales monotonically with strain intensity. If so, it may then be possible to use surface roughness measurements straightforwardly to determine the principal components of the strain tensor (i.e. ε_{11}, ε_{22} and ε_{33}) in each strain mode. A constitutive relationship such as this could be quite useful as a predictive tool in sheet metal forming. For this reason, further studies are in progress to determine the universal nature of these characteristics.

References

1. H. A. Al-Quershi, A. N. Klein and M. C. Fredel: *J. Mater. Process. Technol.*, 2005, **170**, 204–210.
2. 'Standard test methods of tension testing of metallic materials', E-08, ASTM, Philadelphia, PA, USA, 1993.
3. 'Surface texture (surface roughness, waviness and lay)', B46·1, ASME, New York, USA, 2002.
4. The Aluminum Association: 'Aluminum standards and data 2003', 235; 2003, Washington, DC, The Aluminum Association.
5. S. W. Banovic, M. A. Iadicola and T. Foecke: *Metall. Mater. Trans. A*, 2008, **39A**, 2246–2258.
6. F. Barlat, R. C. Becker, Y. Hayashida, Y. Maeda, M. Yanagawa, K. Chung, J. C. Brem, D. J. Lege, K. Matsui, S. J. Murtha and S. Hattori: *Int. J. Plast.*, 1997, **13**, 385–401.
7. A. J. Beaudoin, A. Acharya, S. R. Chen, D. A. Korzekwa and M. G. Stout: *Acta Mater.*, 2000, **48**, 3409–3423.
8. R. Becker and O. Richmond: *Modell. Simul. Mater. Sci. Eng.*, 1994, **2**, 439–454.
9. J. E. Bird and J. L. Duncan: *Metall. Trans. A*, 1981, **12A**, 235–241.
10. J. Dattorro: 'Euclidean distance matrix', in 'Convex optimization and euclidean distance geometry', Chapter 4, 219–314; 2005, Palo Alto, CA, MeBoo Publishing.
11. G. E. Dieter: 'Mechanical metallurgy', 751; 1986, New York, McGraw-Hill.
12. P. J. Diggle and P. J. Ribeiro: 'Model-based geostatistics'; 2007, New York, Springer.
13. T. Foecke, M. A. Iadicola, A. Lin and S. W. Banovic: *Metall. Mater. Trans. A*, 2007, **38A**, 306–313.
14. M. A. Iadicola, T. Foecke and S. W. Banovic: *Int. J. Plast.*, 2008, **24**, 2084–2101.
15. W. B. Lievers, A. K. Pilkey and D. J. Lloyd: *Acta Mater.*, 2004, **52**, 3001–3007.
16. Z. Marciniak and K. Kuczynski: *Int. J. Mech. Sci.*, 1967, **9**, 609–620.
17. W. Meeker and L. A. Escobar: 'Statistical methods for reliability data'; 1998, New York, John Wiley & Sons.
18. J. A. Nelder and R. Mead: *Comput. J.*, 1965, **7**, 308–313.
19. D. Rabbe, M. Sachtleber, H. Weiland, G. Scheele and Z. Zhao: *Acta Mater.*, 2003, **51**, 1539–1560.
20. K. S. Raghavan: *Metall. Mater. Trans. A*, 1995, **26A**, 2075–2084.
21. J. Savoie, M. Jain, A. R. Carr, P. D. Wu, K. W. Neale, Y. Zhou and J. J. Jonas: *Mater. Sci. Eng. A*, 1998, **A257**, 128–133.
22. M. R. Stoudt and J. B. Hubbard: *Philos. Mag.*, 2009, **89**, 2403–2425.
23. M. R. Stoudt, J. B. Hubbard, M. A. Iadicola and S. W. Banovic: *Metall. Mater. Trans. A*, 2009, **40A**, 1611–1622.
24. M. R. Stoudt, J. B. Hubbard and S. A. Janet: *Mater. Sci. Technol.*, 2008, **24**, 253–260.
25. M. R. Stoudt, J. B. Hubbard, S. P. Mates and D. E. Green: *SAE Trans., J. Mater. Manuf.*, 2006, **114**, (5), 183–190.
26. R Development Core Team: 'R: A language and environment for statistical computing', R Foundation for Statistical Computing, Vienna, Austria, 2009.
27. P. D. Wu, D. J. Lloyd, M. Jain, K. W. Neale and Y. Huang: *Int. J. Plast.*, 2007, **23**, 1084–1104.